

## Scale-free brain functional networks

Victor M. Eguíluz,<sup>1</sup> Dante R. Chialvo,<sup>2</sup> Guillermo Cecchi,<sup>3</sup> Marwan Baliki,<sup>2</sup> and A. Vania Apkarian<sup>2</sup>

<sup>1</sup>*Instituto Mediterráneo de Estudios Avanzados, IMEDEA (CSIC-UIB), E07122 Palma de Mallorca, Spain*

<sup>2</sup>*Department of Physiology, Northwestern University, Chicago, Illinois, 60611, USA.*

<sup>3</sup>*IBM T.J. Watson Research Center, 1101 Kitchawan Rd., Yorktown Heights, NY 10598, USA.*

(Dated: January 28, 2020)

Functional magnetic resonance imaging was used to define networks among correlated human brain sites. Analysis of the resulting networks shows: the distribution of functional connections and probability of finding a link vs. distance are both scale-free. The characteristic path length is relatively small and comparable to those calculated for equivalent random networks. The clustering coefficient is orders of magnitude larger than those of equivalent random networks and much larger than that of the null model with random rewiring. Additionally, an unexpected assortative feature was apparent, previously only seen in social networks. All these properties, typical of scale-free small world networks, reflect important functional information about brain states.

PACS numbers:

Recent work has shown that disparate systems can be described as complex networks, that is assemblies of nodes and links with nontrivial topological properties [1, 2, 3], examples include technological, biological and social systems. The brain is inherently a dynamic system, in which the traffic between regions, during behavior or even at rest, creates and reshapes continuously complex functional networks of correlated dynamics. An important goal in neuroscience is to understand these spatio-temporal patterns of brain activity. This letter describes these networks, seen using functional magnetic resonance imaging (fMRI) in humans, analyzed in the context of the current understanding of complex networks (for reviews see [1, 2, 3, 4, 5, 6]). Figure 1 illustrates graphically how the underlying functional networks are exposed during any given task. In these experiments, at each time step (typically 400 spaced 2.5 sec.), magnetic resonance (MR) brain activity is measured from  $36 \times 64 \times 64$  brain sites (so-called “voxels” of dimension  $3 \times 3.475 \times 3.475 \text{ mm}^3$ ). The activity of voxel  $x$  at time  $t$  is denoted as  $V(x, t)$ . We define here as functionally connected those brain sites whose temporal evolution are correlated beyond a positive pre-established value, an approach used previously [7], but networks can be built as well by defining negative or positive correlations. Specifically, we calculate the linear correlation coefficient between any pair of voxels,  $x_1$  and  $x_2$ , as:

$$r(x_1, x_2) = \frac{\langle V(x_1, t)V(x_2, t) \rangle - \langle V(x_1, t) \rangle \langle V(x_2, t) \rangle}{\sigma(V(x_1))\sigma(V(x_2))}, \quad (1)$$

where  $\sigma^2(V(x)) = \langle V(x, t)^2 \rangle - \langle V(x, t) \rangle^2$ , and  $\langle \cdot \rangle$  represent temporal averages. Thus, as depicted in Fig. 1 the network is extracted by defining a threshold  $r_c$  for the correlation matrix. Of course, if one chooses a value of  $r_c$  that is too small, then the majority of the voxels will appear to be connected to one another. Likewise if the

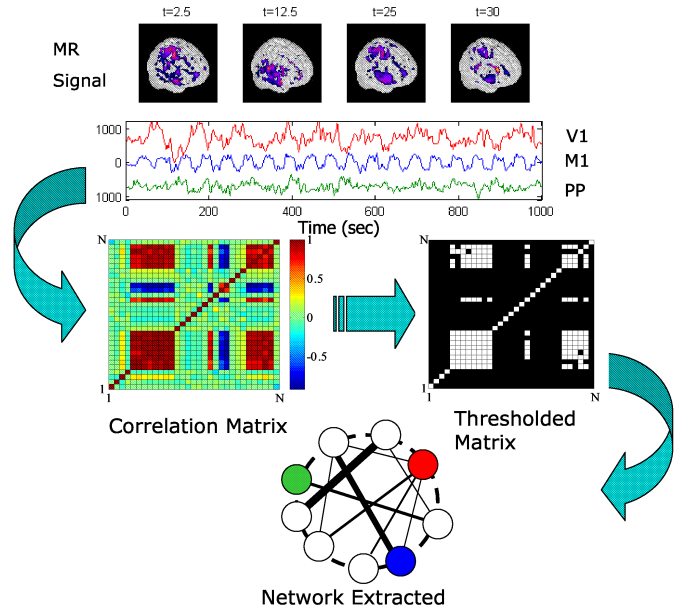


FIG. 1: Methodology used to extract the networks from the signals. The correlation matrix is calculated and then used to define the network among the highest correlated nodes. Top four images represent snapshots of activity and the three traces correspond to selected voxels from visual (V1), motor (M1) and postero-parietal (PP) cortices.

threshold is too high, then voxels will appear isolated. Empirically, we have found that there is a wide range of threshold values for which networks remain clearly defined indicating that the main conclusions are robust with respect to the selection of parameters. Figure 2 shows an example of a network extracted using this method. (Data collected while the subject was opposing fingers 1 and 2 during 10 seconds, and then resting during 10 sec.). For clarity, only one eighth of the nodes are included in the illustration. The pattern of inhomogeneous

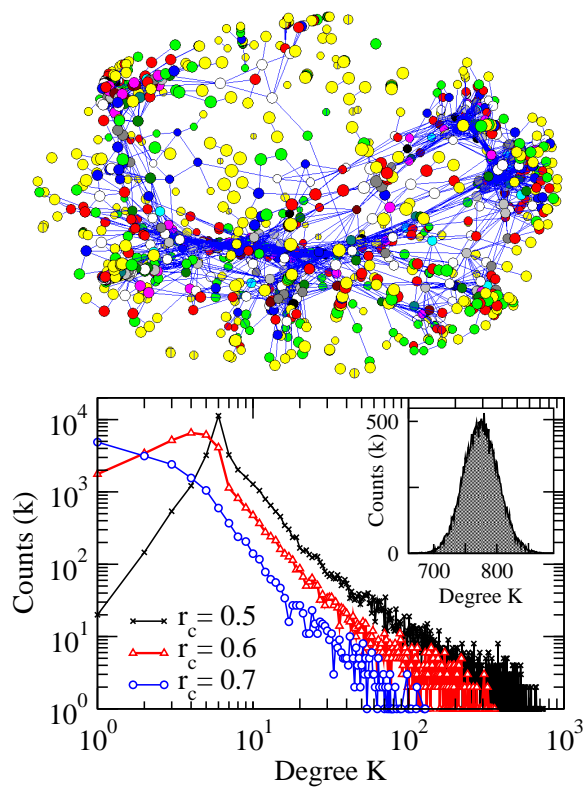


FIG. 2: Example of a network extracted using the methods described in Fig. 1. Top panel shows a pictorial representation of the network (Nodes colored according to its degree: yellow = 1, green = 2, red = 3, blue=4, etc). The bottom panel shows the degree distribution for three values of the correlation threshold. The inset depicts the degree distribution for an equivalent randomly connected network.

connectivity is visually evident. One sees a relatively large proportion of nodes with a single link (colored yellow) and a smaller proportion of nodes with numerous connections. A quantitative estimate of this inverse relationship is shown in the bottom panel of Fig. 2. We find a skewed distribution of links with a tail approaching a distribution  $p(k) \sim k^{-\lambda}$ , with  $\lambda$  around 2. This power law is more evident for networks constructed with higher thresholds  $r_c$  (more correlated conditions). (For decreasing  $r_c$ , a maximum appears which shifts to the right). The functional networks are scale-free. The small inset in Fig. 2 shows the distribution of links of a surrogate network constructed from the randomly shuffled (in time) voxels signal. The degree distribution of these networks displays a Gaussian distribution in which the mean and width depend on  $r_c$ . The largest values of the correlation thresholds used to construct the random networks are usually extremely low ( $r_c \sim 0.1$ ) compared to that used to define the raw networks ( $r_c \sim 0.7$ ). Our data were also compared with values from a randomly re-wired network, where nodes with similar degrees are permuted (i.e., the link connecting nodes  $i, j$  is permuted with that connecting nodes  $k, l$ ) as introduced by Maslov

et al. [8](see below). In this control the degree is maintained but all other correlations (including clustering) are destroyed.

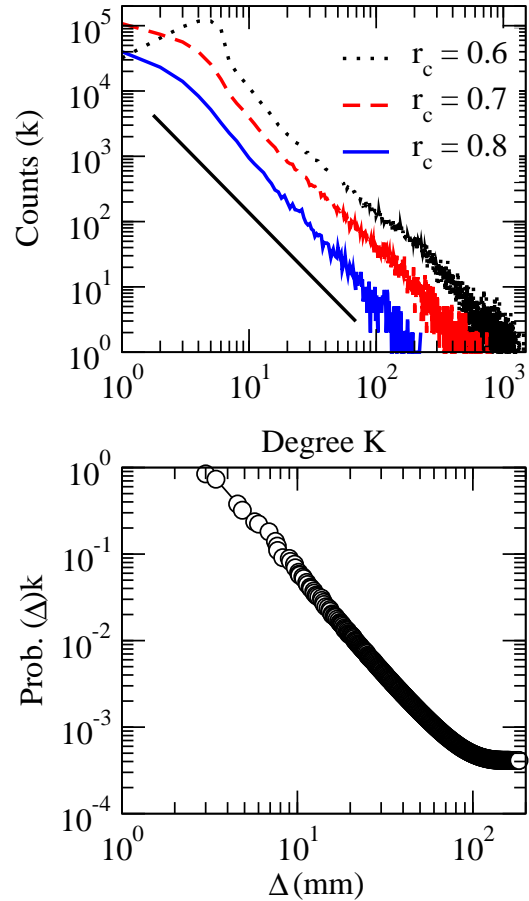


FIG. 3: Average scaling taken from 22 networks extracted from seven subjects. Top Panel: Average degree distribution. The straight line illustrates a decay of  $k^{-2}$ . Bottom panel: Average probability of finding a link between two nodes separated by a distance  $x < \Delta$  (using  $r_c = 0.6$ ).

To test the generality of these findings similar analysis was performed in 7 subjects across 3 task conditions. During the data acquisition[9] the subjects perform on-off finger tapping with three different protocols. In one case is instructed verbally to start and stop tapping, in the other one the clue is a small green/red dot in a video screen and in the last one the clue is the entire screen turning green or red. The results are very robust across subjects and task conditions. In particular, the average of degree distribution (see Fig. 3) shows a clear power law scaling decaying as  $p(k) \sim k^{-\lambda}$ , with an exponent close to 2. Although a precise fitting is arguably difficult, we find that for  $r_c=0.6$   $\lambda = 2$ , for  $r_c=0.7$  is 2.1 and for  $r_c=0.8$  is 2.2. This power law implies that there is always a small but finite number of brain sites that have broad “access” to most other brain regions. Those well connected nodes are comparatively much more numerous in these networks than in a randomly connected network.

$r_c$	$N$	$C$	$L$	$\langle k \rangle$	$\lambda$	$C_{rand}$	$L_{rand}$
0.6	31503	0.14	11.4	13.41	2.0	$4.3 \times 10^{-4}$	3.9
0.7	17174	0.13	12.9	6.29	2.1	$3.7 \times 10^{-4}$	5.3
0.8	4891	0.15	6.	4.12	2.2	$8.9 \times 10^{-4}$	6.0

TABLE I: Average statistical properties of the brain functional networks.

<i>Network</i>	$N$	$C$	$L$	$\langle k \rangle$	$\lambda$	$C_{rand}$	$L_{rand}$
C. Elegans	282	0.28	2.65	7.68	NA	0.025	2.1
Macaque VC	32	0.55	1.77	9.85	NA	0.318	1.5
Cat Cortex	65	0.54	1.87	17.48	NA	0.273	1.4

TABLE II: Previously reported statistics of relatively smaller networks. Because these networks are not scale-free  $\lambda$  is not indicated.

Importantly, we have verified that although the network engages different brain regions across varying task conditions, the scale-free character remains in all cases. As shown in the bottom panel of Fig. 3 the average probability of finding a link between two nodes, separated at least by a distance  $x$ , also decays as a power law. The significance of the scaling with distance is unclear because of the well known extensive cortex folding, which makes linear distance a dubious parameter. Path length and clustering are also important statistical properties of networks. The path length ( $L$ ) between two voxels is the minimum number of links necessary to connect both voxels. Clustering ( $C$ ) is the fraction of connections between the topological neighbors of a voxel with respect to the maximum possible. If voxel  $i$  has degree  $k_i$ , then the maximum number of links between the  $k_i$  neighbors is  $k_i(k_i - 1)/2$ . Thus, if  $E_i$  is the number of links connecting the neighbors then the clustering of voxel  $i$ ,  $C_i = 2E_i/k_i(k_i - 1)$ . The average clustering of a network is given by  $C = 1/N \sum_i C_i$ , where  $N$  is the number of voxels. Clustering was analyzed also with respect to degree. The average clustering over voxels with the same degree  $C(k) = 1/N_k \sum_{j=\{i|k_i=k\}} C_j$ , where the sum runs over the  $N_k$  voxels with degree  $k$ .

Table 1 summarizes the results for the networks analyzed showing the average values ( $n = 22$  datasets) for each threshold ( $r_c$ , first column) used to construct the networks. Listed are  $N$ ,  $C$ ,  $L$ , the average degree  $\langle k \rangle$ , and  $\lambda$ . The clustering ( $C_{rand}$ ) and path length ( $L_{rand}$ ) values of an equivalent random network are also included for comparison. Note that as the threshold  $r_c$  increases the total number of nodes  $N$  decreases substantially, resulting by definition in more correlated networks. As a result, the number of nodes with at least one link decreases, and consequently the  $\langle k \rangle$  value decreases as well. In all cases, the coefficient  $C$  remains four orders of magnitude larger than  $C_{rand}$ , the clustering of a random network. Networks randomized using the rewiring

described by Maslov et al. [8] also have clustering significantly smaller than the raw data (the order of  $10^{-2}$ ). This feature, together with the similarity of path length of the original nets and their randomized controls ( $L$  and  $L_{rand}$ ), is indicative of a small-world structure [5, 6]. Note that this property is robust as it does not depend critically on the numerical parameter  $r_c$  used to unveil the network. To our knowledge, this is the first report on the scale-free structure of a large scale brain network. Previous studies employing these statistical analyses have been limited to analysis of the small data sets of C. Elegans [6], or of two neuro-anatomical databases [10, 11, 12], the macaque visual cortex [13] and the cat cortex [14]. These did not demonstrate scale-free features. It is illustrative to contrast the main quantitative conclusions of these reports (condensed in Table 2) with the present results. Firstly, the present methodology allows us to build and analyze networks that are orders of magnitude larger in size. In that sense this paper describes the largest biological network in the literature. With this caveat in mind, comparison with the previous two reports indicate the following: Although clustering in the present study is smaller in absolute value, it is still orders of magnitude larger than the random case ( $10^{-1}$  vs.  $10^{-4}$ ), while in the previous reports the clustering of the experimental data was just one order of magnitude larger than the randomized controls in the best case. Interestingly the average connectivity  $\langle k \rangle$  in all cases is of the same order, despite the huge differences in networks' origins and sizes. Accordingly, this consistency may reflect some constraint(s) inherent to network construction. Taken together these quantitative features show that the human brain network examined here has small world properties, a finding that was previously postulated [5, 6]. Figure 4 illustrates the dependence of two important features upon a voxel's degree. The first is clustering, which has been found in many complex networks to scale as  $C(k) \sim k^{-\alpha}$ , an indication of hierarchical organization [15, 16]. However we have not found this relationship in this case. Rather we see a relative independence of clustering from degree. The second feature is that a highly connected node tends to connect with other well connected nodes. As shown in the bottom panel of Figure 4, the network examined here shows a positive correlation between the degrees of adjacent vertices. The presence of such a correlation, also called assortative mixing, is not typical of biological networks, but rather is distinctive of social networks [17, 18]. In summary, we report statistical measures showing that the functional correlations of the human brain form a scale-free network with small world properties and assortative mixing. While some of these properties have been informally discussed, this work is the first quantitative demonstration of these large-scale topological properties, as well as the first report of an assortative biological network. The scaling laws demonstrated here are

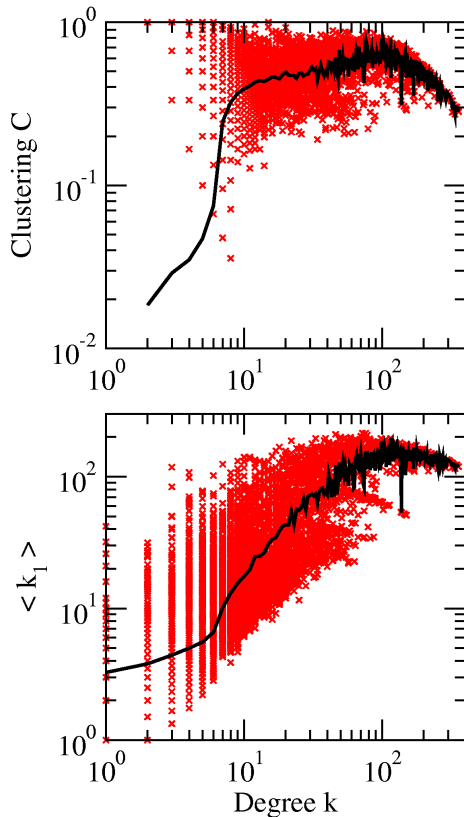


FIG. 4: Top Panel: Plot of clustering vs. degree. Bottom panel: Plot of a neighboring node's degree vs. degree illustrates the assortative feature. Symbols represents individual data and continuous lines the average values for nodes with the same degree. (Same subject shown in Fig. 2, with  $r_c=0.6$ ).

robust across subjects, task conditions and parameters, suggesting they are invariant properties of an underlying network. The present results complement the extensive work done in the context of brain functional and effective connectivity [20, 21]. The present approach has additional important implications. Namely, these studies can be extended to cases in which standard fMRI techniques cannot be used for lack of subject cooperation, (e.g., Alzheimer's patients). Because scale-free complex networks are known to show resistance to failure, facility of synchronization, and fast signal processing [22], it would be important to see whether brain networks scaling properties are altered under various pathologies. In that regard, techniques for investigation of communities' structures [23], developed for other networks, should be useful to analyze these aspects. Work on models [24], is needed to further clarify specific origins of the scaling laws. Overall, the network properties uncovered here, offers a novel window to investigate the dynamics of brain states particularly in cases of dysfunction.

**Acknowledgements** We thank financial support from MCyT of Spain (Project BFM2002-04474-C02-01) and NIH NINDS of USA (Grants 42660 and 35115). DRC

is grateful for the hospitality and support of the Universitat de les Illes Balears, Palma de Mallorca, Spain.

- 
- [1] Albert R. and Barabasi A.-L. *Rev. Mod. Phys.* 74, 47 (2002).
  - [2] Newman, M.E.J. *SIAM Review* 45, 167-256 (2003).
  - [3] Jasny BR and Ray LB, *Science* 301:1863 (2003).
  - [4] Dorogovtsev S. N. and Mendes J. F. F. *Adv. Phys.* 51, 1079 (2002)
  - [5] Strogatz S.H, *Nature* 410, 268-276 (2001).
  - [6] Watts D.J. and Strogatz S.H. *Nature* 393, 440-442 (1998).
  - [7] Dodel S., Herrmann JM and Geisel T. *Neurocomputing* 44, 1065-1070 (2002).
  - [8] Maslov S., Sneppen K., and Alon U. In *Handbook of graphs and networks. From the genome to the internet* (Eds S. Bornholdt and H.G. Schuster) 169-198. (Wiley -VCH and Co. Weinheim, 2003).
  - [9] Seven healthy, right-handed human subjects were studied using a Siemens-Trio 3.0 Tesla whole-body imaging system using a birdcage radio-frequency head coil. Blood oxygenation level-dependent single-shot echo-planar T2-weighted imaging was obtained using scan repeat time of 3000 ms, echo time of 30 ms, flip angle 90, field 256 mm. The data were preprocessed using the package FEAT [25] and motion correction done using MCFLIRT [26]. All procedures employed were approved by Northwestern University Institutional Review Board.
  - [10] Sporns O., Tononi G. and Edelman G.M. *Cerebral Cortex* 10, 127-141, (2000).
  - [11] Sporns O. and Tononi G. *Complexity* 7, 28-38 (2003).
  - [12] Hilgetag, CC, Burns, G. A. P. C. and O'Neill, M. A. and Scannell, J. W. and Young, M. P, *Phil. Trans. R. Soc. Lond. B* 355,91-110 (2000).
  - [13] Felleman D.J. and Van Essen D.C. *Cerebral Cortex* 1, 1-47 (1991).
  - [14] Scannell J.W., Burns G.A.P.C., Hilgetag C.C., O'Neill M.A. and Young M.P. *Cerebral Cortex* 9, 277 (1999).
  - [15] Ravasz E. and Barabasi A.-L. *Phys. Rev. E* 67, 026112 (2003).
  - [16] Jeong H, Mason SP, Barabasi A-L and Oltvai ZN. *Nature* 411, 41-42 (2001).
  - [17] Newman M. E. J. *Phys. Rev. Lett.* 89, 208701 (2002)
  - [18] Newman M.E. J., Park J. *Phys. Rev. E* 68, 036122 (2003)
  - [19] Bogua M., Pastor-Satorras R., Daz-Guilera A., and Arenas A. E-print cond-mat/0309263.
  - [20] Biswal B, Yetkin FZ, Haughton VM, Hyde JS. *Magn Reson Med.* 34(4):537-41.(1995).
  - [21] Friston KJ, In: *Brain Mapping The Methods*, Eds. Toga and Mazziotta, 2nd edition, Chapter 22, (2002).
  - [22] Lago-Fernandez LF, Huerta R, Corbacho F, Siguenza JA. *Phys. Rev. Lett.* 84, 2758-2761 (2000).
  - [23] Radicchi F., Castellano C., Cecconi F., Loreto V., Parisi D. E-print cond-mat/ 0309488.
  - [24] Caldarelli G., Capocci A., De Los Rios P., Muoz M.A. *Phys. Rev. Lett.* 89, 258702 (2002).
  - [25] Smith S.M., De-Stefano N., Jenkinson M. and Matthews P.M. *J. Comput. Assist. Tomogr.* 25, 466-475, (2001).
  - [26] Jenkinson M. and Smith S. *Med. Image Anal.* 5, 143-156 (2001).